Response of bacterial colonies to imposed anisotropy

Eshel Ben-Jacob, Ofer Shochet, Adam Tenenbaum, and Inon Cohen
School of Physics and Astronomy, Raymond and Beverly Sackler Faculty of Exact Sciences, Tel Aviv University, Tel Aviv 69978, Israel

Andras Czirók and Tamas Vicsek
Department of Atomic Physics, Eötvös University, Budapest, Puskin u 5-7, 1088 Hungary
(Received 12 September 1994)

We present theoretical and experimental studies of bacterial growth patterns in the presence of imposed anisotropy. The role of chemotactic signaling in the cooperative response of the bacteria is demonstrated. In the presence of sixfold symmetry, patterns with a tantalizing similarity to those of snowflakes are formed. Transitions from concave to convex shaped envelope as a function of peptone level are observed in the presence of fourfold lattice anisotropy.

PACS number(s): 87.22.−q, 61.43.Hv, 02.60.Cb

I. INTRODUCTION

Many natural phenomena, in living and nonliving systems alike, display the spontaneous emergence of patterns; growth of snowflakes, aggregation of soot particles, solidification of metals, formation of corals, growth of bacterial colonies, and cell differentiation during embryonic development are just a few. The exciting developments of the past decade in the understanding of diffusive patterning in nonliving systems [1–4] contain a promise for a unified theoretical framework (for nonliving systems) that might also pave the road toward a new understanding of processes in living systems.

In nature bacterial colonies must regularly cope with hostile environmental conditions [5,6]. We produced hostile conditions in a Petri dish by using a very low level of nutrients, a hard surface (high concentration of agar), or both, together with a new element — imposed anisotropy. Drawing on the analogy with diffusive patterning in nonliving systems, complex patterns are expected. The bacterial reproduction rate, which determines the growth rate of the colony, is limited by the nutrient concentration. The latter is limited by the diffusion of nutrients towards the colony. Hence the growth of colonies appears to resemble diffusion limited growth in nonliving systems, such as solidification from a supersaturated solution, electrochemical deposition, etc. [3,4]. Indeed, bacterial colonies do develop patterns reminiscent of those observed during growth in nonliving systems [7–12]. Still, one should not conclude that complex patterning of bacterial colonies is yet another example (albeit more involved) of spontaneous emergence of patterns, which may be explained according to the theory of patterning in nonliving systems.

The bacteria present an inherent additional level of complexity compared to nonliving systems [7,9,10,13–15]. The building blocks of the colony are themselves living systems, each with its own autonomous self-interest and internal degrees of freedom. At the same time, efficient adaptation of the colony to adverse growth conditions requires self-organization on all levels — which can be achieved only via cooperative behavior of the bacteria [11,16,17]. To do so, the bacteria have developed sophisticated communication channels on all levels [18–23]: Those include direct (by contact) bacterium-bacterium physical interaction and chemical interaction, and indirect physical and chemical interactions via marks left on the agar surface and chemical signaling (chemotactic). For researchers in the pattern formation field, the above communication regulation and control mechanisms present a new class of challenging problems [15,16,24,25].

An essential part of the new understanding of diffusive patterning in nonliving systems has to do with the role of anisotropy [1–4]. The latter is responsible for the appearance of dendritic growth rather than a cascade of tip splitting. What would be the response of a colony grown under diffusion limited conditions to imposed anisotropy or to a local broken symmetry in the growth conditions? From the lesson learned from nonliving systems we expect the imposed modulation to act as a singular perturbation: a qualitative change in the shape of the colony even for minute perturbation. Hence the tip-splitting growth will turn into a dendritic growth characterized by a stable leading tip with a parabolic shape, as indeed is demonstrated in Fig. 1.

Here we study both experimentally and theoretically — using the communicating walkers model — the effect of two types of imposed anisotropy. The first is a six-fold line anisotropy, in which the surface is modulated along three intersecting lines (the diagonals of a hexagon). The second is a fourfold lattice anisotropy, in which the surface is modulated along two sets of parallel lines, where the sets are perpendicular to each other and form a fourfold lattice. In both cases we study theoretically the effect of repulsive chemotaxis. For the sixfold line anisotropy we show that the effect of the anisotropy fades away at low peptone levels unless chemorepulsion is included in the model. In the case of fourfold lattice anisotropy we show a concave to convex transition (as a

function of peptone level) when repulsive chemotaxis is included in the model. We emphasize that the qualitative differences between the two cases of anisotropies are not due to the degree of symmetry. Rather, they result from the fact that the first case is a line anisotropy and in the second case a lattice is imposed.

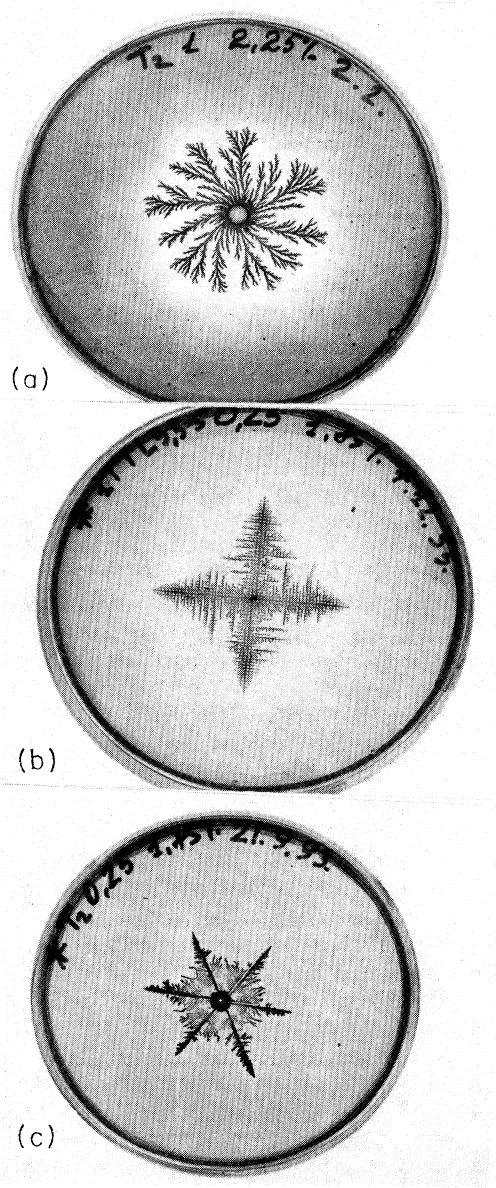

FIG. 1. The effect of imposed anisotropy. (a) Fractal growth in the absence of anisotropy on 2.25% agar (1% is 1 g per 100 ml) and 1 g/l peptone level. (b) Dendritic growth in the presence of imposed fourfold lattice anisotropy. The anisotropy is introduced using the "stamping" method described in the text. The growth is for 0.25 g/l peptone level and 1.75% agar concentration. Note the dramatic effect of the imposed anisotropy and the tantalizing similarity to solidification patterns and patterns produced in Hele-Shaw experiments. (c) "Bacterial snowflake," the same as (b) but in the presence of sixfold anisotropy.

II. THE "COMMUNICATING WALKERS" MODEL

For the theoretical investigations we have employed the "communicating walkers" model [15]. The communicating walkers model is a hybridization of the "continuous" and "atomistic" approaches used in the study of nonliving systems [26]. The diffusion of the chemicals is handled by solving a continuous diffusion equation (including sources and sinks) on a triangular lattice, while bacteria are represented by walkers allowing a more detailed description. In a typical experiment there are 10^9–10^{10} bacteria in a Petri dish at the end of the growth. Hence it is impractical to incorporate into the model each and every bacterium; instead, each of the walkers represents about 10^4–10^5 bacteria, so that we work with 10^4–10^6 walkers in one run.

The walkers perform random walks on a plane within an envelope representing the boundary of the wetting fluid. This envelope is defined on the same triangular lattice where the diffusion equations are solved. To incorporate the swimming of the bacteria into the model, at each time step each of the active walkers (motile and metabolizing, as described below) moves a step of size d at a random angle Θ. Starting from location $\vec{r}_i$, it moves

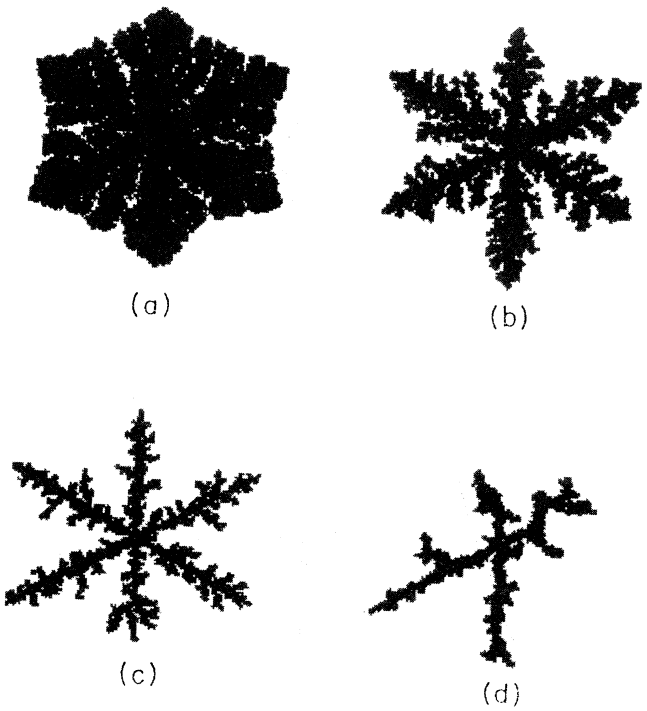

FIG. 2. Patterns produced by the "communicating walkers" model in the presence of imposed sixfold anisotropy. The simulations are for N_c=10. (a)–(d) are for P=50, 20, 10, and 5, respectively. At high peptone levels the pattern is dense and the sixfold modulation is weak. At intermediate values of peptone level the anisotropy is most pronounced. At very low peptone the patterns are ramified and the sixfold symmetry is lost.

to a new location $\vec{r}_i'$ given by

$$\vec{r}_i' = \vec{r}_i + d(\cos\Theta; \sin\Theta) \ . \tag{1}$$

If $\vec{r}_i'$ is outside the envelope, the walker does not move. A counter on the segment of the envelope which would have been crossed by the movement $\vec{r}_i \to \vec{r}_i'$ is increased by 1. When the segment counter reaches a specified number of hits N_c, the envelope propagates one lattice step and an additional lattice cell is added to the colony. This requirement of N_c hits represents the colony propagation as the bacteria push the wetting fluid. Note that N_c is related to the agar concentration, as more wetting fluid must be produced (more "collisions" are needed) to push the envelope on a harder substrate.

We represent the metabolic state of the ith walker by an "internal energy" E_i. The rate of change of the internal energy is given by

$$\frac{dE_i}{dt} = \kappa C_{consumed} - \frac{E_m}{\tau_R} \ , \tag{2}$$

where κ is a conversion factor from food to internal energy ($\kappa \cong 5 \times 10^3$ cal/g) and E_m represents the total energy loss for all processes over the reproduction time τ_R, excluding energy loss for cell division. $C_{consumed}$ is

$$C_{consumed} \equiv \min(\Omega_C, \Omega_C') \ , \tag{3}$$

where Ω_C is the maximal rate of food consumption if enough food is available. Otherwise the walker consumes food at a rate Ω_C' which is the maximal rate of food consumption as limited by the locally available food [27].

When sufficient food is available, E_i increases until it reaches a threshold energy. Upon reaching this threshold, the walker divides into two. When food is deficient for an interval of time, causing E_i to drop to zero, the walker "freezes."

Although the food source in our experiments is peptone (and not a single carbon source), we represent the diffusion of nutrients by solving the diffusion equation for a single agent whose concentration is denoted by $C(\vec{r}, t)$:

$$\frac{\partial C}{\partial t} = D_C \nabla^2 C - \sigma C_{consumed} \ , \tag{4}$$

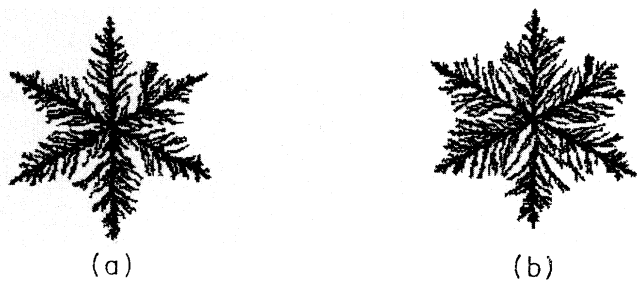

FIG. 3. The effect of repulsive chemotaxis. (a) and (b) are the same as Fig. 2(d) but with repulsive chemotaxis [stronger in (b)]. The pattern becomes dense and the anisotropy is retained.

where the last term includes the consumption of food by the walkers (σ is their density). The equation is solved on the triangular lattice. We start the simulation with a uniform distribution C_0 (denoted in the figures by P for peptone; $P = 10$ corresponds approximately to $1g/l$). The diffusion constant D_C is typically (depending on agar dryness) 10^{-4}–10^{-6} cm^2/sec.

We have proposed that chemotaxis signaling plays a crucial role in the cooperative formation of complex bacterial patterns [15,27–29]. Generally, chemotaxis means a change in the movement of the bacteria in response to a gradient of certain chemical field [23,30,31]. The movement is biased along the gradient either in the gradient direction or in the opposite direction. Usually, a chemotactic response means a response to an externally produced field as in the case of food chemotaxis. However, the chemotactic response may also be to a field produced directly or indirectly by the bacteria. We will refer to this as chemotaxis signaling. As we will show, it provides an effective means for self-organization of the colony.

In Refs. [27,32] it is proposed that the wealth of observed bacterial patterns is attained by varying the relative strength of three kinds of chemotactic signaling [28]: a long-range nutrient chemotaxis, a long-range repulsive signaling chemotaxis, and a short-range autocatalytic chemoattraction. The interplay between the three kinds of chemosignaling provides the colony with means

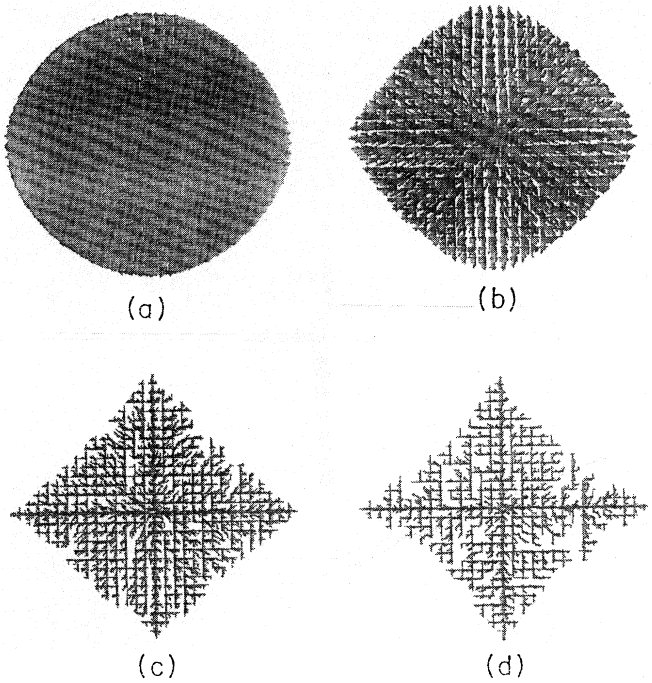

FIG. 4. Patterns produced by the "communicating walkers" model in the presence of lattice fourfold anisotropy and with chemotaxis signaling. The simulations are for N_c=20. (a)–(d) are for P=75, 35, 15, and 10, respectively. Note that the envelope shows a transition from concave to convex shape envelope.

for self-organization, at both short and long range. The balance is tuned by the bacteria in response to the environmental conditions. Here we focus on the behavior at low peptone levels so we include only the chemorepulsive signaling.

We assume [15] that the stressed bacteria inside the colony emit a chemorepellent. That is, under starvation bacteria emit a material (either purposely or as a by-product of an adaptation process) that causes other bacteria to move away.

The equation describing the concentration field $R(\vec{r},t)$ of the chemorepellent is

$$\frac{\partial R}{\partial t} = D_R \nabla^2 R + \sigma^* P_R - R_{consumed}, \tag{5}$$

where σ^* denotes the density of stressed walkers, and $R_{consumed}$ is given by $\min\left(\Omega_R \sigma, R\right)$ expressing that the decomposition of R is limited by a maximal rate Ω_R.

III. THE EFFECT OF IMPOSED ANISOTROPY

We turn now to study the effect of imposed anisotropy, using the communicating walkers model. To introduce sixfold line anisotropy we simply set lower N_c values along six specified stripes. Results of numerical simulations of the model in the presence of anisotropy are shown in Fig. 2. The patterns show a tantalizing similarity to the shape of snowflakes. There is a pronounced sixfold symmetry with leading dendritic tips, from which side branches are emitted, forming a denser pattern for high peptone levels. At very low peptone the sixfold symmetry is lost and the patterns become very ramified. However, when repulsive chemotaxis signaling is included, the patterns at low peptone level become dense and the sixfold symmetry is retained as is shown in Fig. 3.

Next, we have studied the effect of imposed fourfold lattice anisotropy. In nonliving systems, the individual stems of the growing patterns are organized to form a well defined shape-preserving envelope which propagates at a constant velocity. Shochet *et al.* [26,33] have demonstrated that there is a concave-to-convex transition in the shape of the envelope as we vary the driving force (supersaturation or undercooling for solidification), indicating the existence of a morphology selection principle. Would a similar transition be observed during growth of bacterial colonies? In Fig. 4 we show simulations of the communicating walkers model in the presence of fourfold lattice anisotropy. The anisotropy is included via a four-fold net of lines along which N_c is of lower value. The results show a clear concave-to-convex transition as a function of peptone level. Chemotaxis signaling has been included in the simulations shown in Fig. 4. In the absence of such signaling, the concave-to-convex transition fades away.

IV. "BACTERIAL SNOWFLAKES"

To test the above predictions, we have looked for a method to impose controlled weak broken symmetry on the agar surface of bacteria grown in Petri dishes (the experimental procedure is described in Refs. [9,10]). Previously [9] we have observed dendritic growth in response to uncontrolled (spontaneous) anisotropy which is formed during drying of the agar. We looked for controlled anisotropy, one that can be mimicked in the model's simulations. In the case of solidification, the anisotropy is provided by the symmetry of the crystalline structure of the growing phase (the solid). In Hele-Shaw experiments, anisotropy was imposed via grooved channels on one of the plates [34,35]. In other Hele-Shaw experiments, anisotropy was imposed locally at the growing

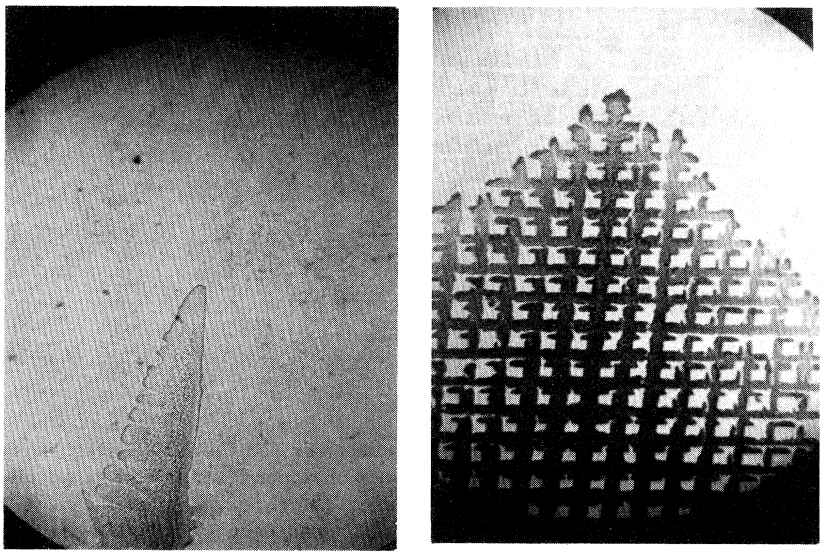

FIG. 5. Close-up picture of the imposed anisotropy (× 50 magnification) showing the marks left on the agar. (a) Imposed sixfold anisotropy. A segment of one of the six lines is shown. In this case the agar was stamped with wide channels (about 0.6 mm) leading to the growth of parity-broken dendrites (see text). (b) Imposed fourfold mesh anisotropy.

tip via small droplets [36] or by inserting a string in the fluid [37].

After experimenting with various approaches, we have found the following method of "agar stamping" to be most efficient. The stamp is a cylindrical Plexiglas bar (7 cm in diameter and 7 cm in height). On one face of the cylinder we groove six channels 0.8 mm wide and 0.5 mm deep. The agar is stamped after it has been dried for three days, losing 8% of its weight. The stamping is performed by placing the Petri dish face down on the stamp and placing another Plexiglas bar on the back of the Petri dish for 10 sec. This process induces modulation on the agar surface (Fig. 5). Each of the stamp's channels leaves a weak range of elevated agar (less than 0.1 mm). The agar is softer along the top of the ridges. This effect (which is the analog of anisotropy in surface tension) is captured by the model (variations in N_c). There is also an imposed curvature along the two sides of the ridges. This effect, which is the analog of anisotropy in surface kinetics, is not included in the model at present. It leads (as we will show elsewhere) to growth of parity-broken dendrites for wide ridges.

In Fig. 6 we show typical growth patterns observed during growth in the presence of imposed sixfold anisotropy. The patterns exhibit a tantalizing similarity to the shapes of real snowflakes. Each morphology consists of six main arms with either (according to the growth conditions) parabolic tips similar to that of ordinary dendrites [1–4,38] [Fig. 7(a)] or half parabolic tips similar to that of parity-broken dendrites [39–42] [Fig. 7(b)]. At high peptone levels, the patterns are denser and the effect of the anisotropy fades away. At

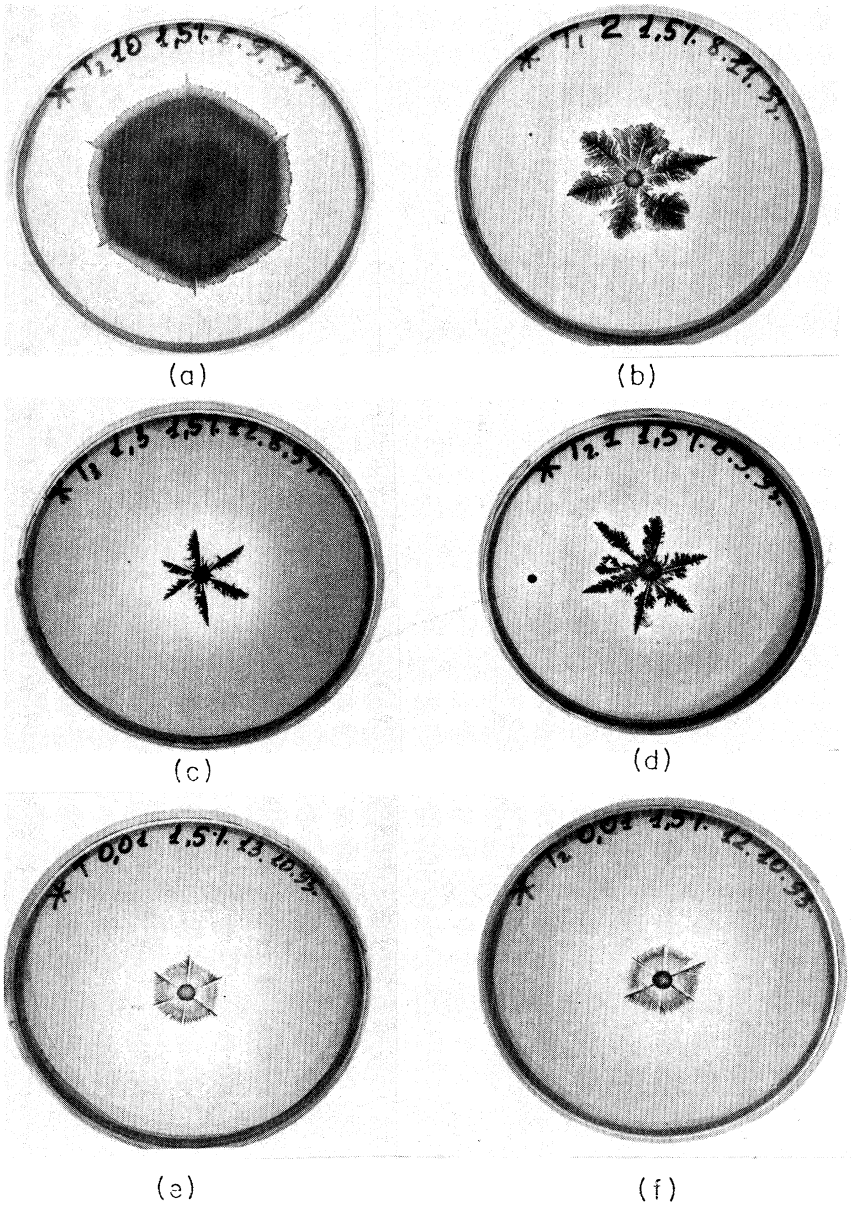

FIG. 6. Patterns observed during growth in the presence of sixfold anisotropy on 1.5% agar concentration and for 10, 2, 1.3, 1.0, 0.01, and 0.01 g/l peptone levels for (a), (b), (c), (d), (e), and (f), respectively. Note that the patterns become denser again at very low peptone levels. The patterns in (e) and (f) (both for the same growth conditions) demonstrate the reproducibility of our results when a strict protocol is followed.

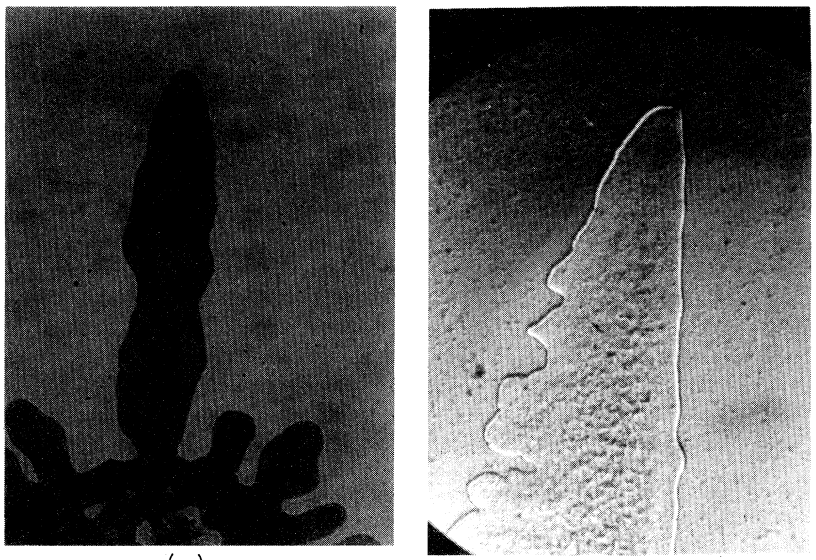

FIG. 7. Close-up look (× 50 magnification) at dendritic growth. (a) Ordinary dendrite with parabolic tip (growth in the presence of twofold anisotropy). (b) Parity-broken dendrite (in the presence of sixfold anisotropy). Note that it appears as "half" of an ordinary dendrite.

very low peptone levels, the patterns become denser again and maintain the sixfold symmetry, in agreement with the simulations when repulsive chemotaxis is included.

The observations demonstrate that singular perturbation does play a role during growth of bacterial colonies. The modulations on the agar surface break the symmetry in the dynamics over just a small regime of the advancing front in the immediate vicinity of the ridge. Yet this broken symmetry is sufficient to change the original tip-splitting growth into dendritic growth. Moreover, the observed dense structure at very low peptone levels provides additional support for the hypothesis that a repulsive chemotactic signaling is employed by the bacteria for better adaptation to the growth conditions.

V. "BACTERIAL CRYSTALS"

Next, we present observations of growth in the presence of fourfold lattice anisotropy. Here we stamp the agar with a Plexiglas cylinder on which a set of parallel channels is grooved. The agar is stamped twice, while the Plexiglas cylinder is rotated by 90° between the two stamps, to produce the lattice mesh shown in Figs. 5 and 8. In Fig. 9 we show the level of reproducibility which is obtained when a strict protocol of stamping the agar is followed. The growth pattern is sensitive to the nature of

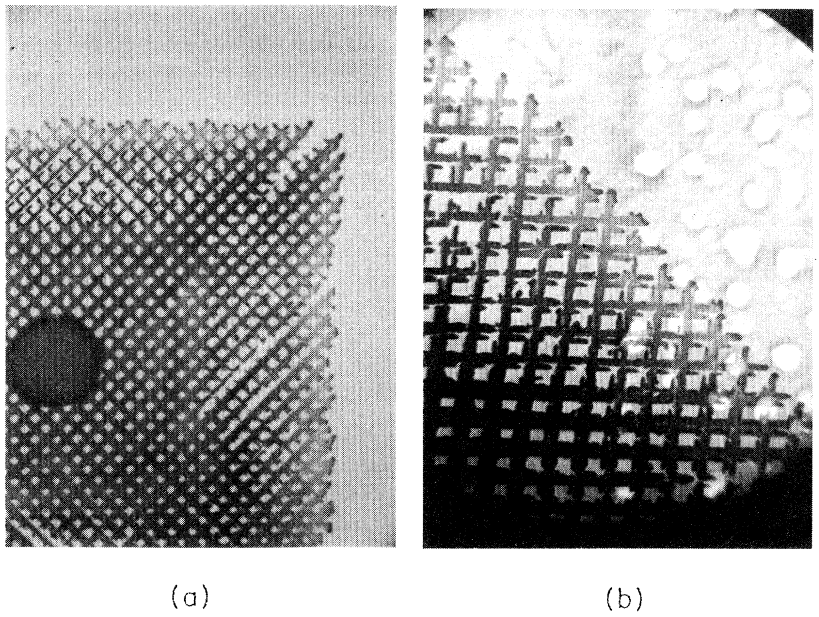

FIG. 8. "Bacterial crystals": growth in the presence of fourfold anisotropy. Note the well defined envelope of the growth. (b) Shows a close look at a segment of (a).

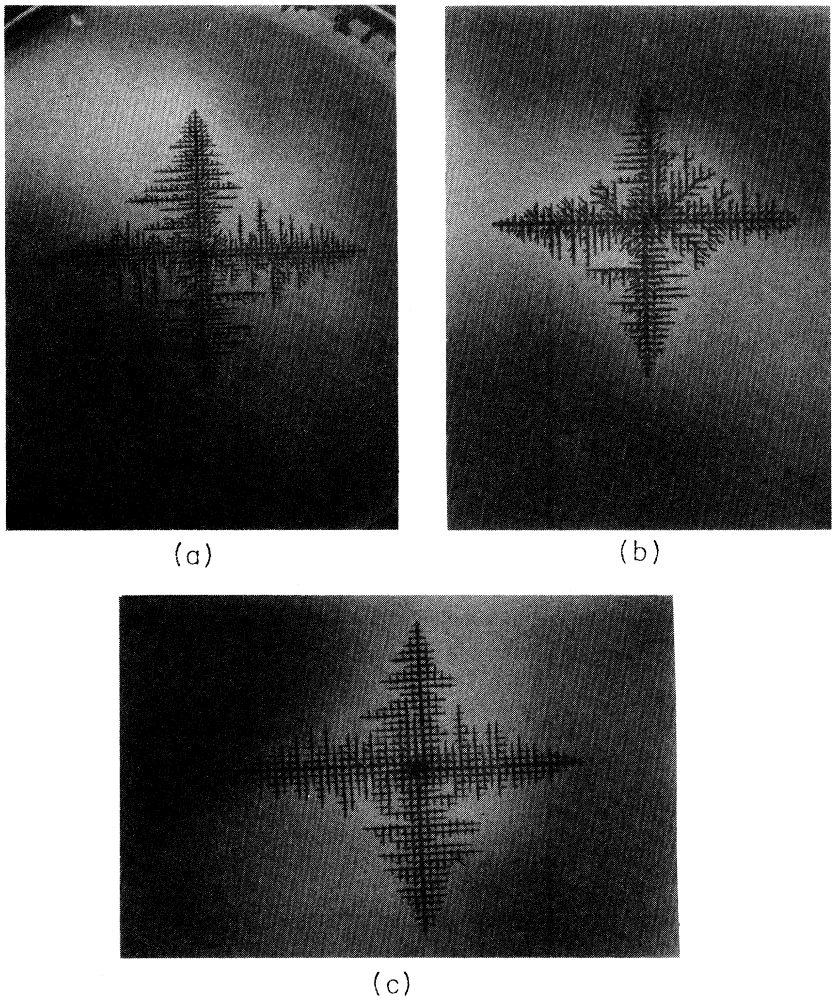

FIG. 9. Demonstration of the reproducibility in the observations. (a), (b), and (c) are for 1.75% agar concentration and 0.25 g/l peptone level. The differences in size are an artifact of the photography. The actual size is the same in all three cases. Note the transient effects near the center of the growth which are due to the initial inoculation (by picking in the center).

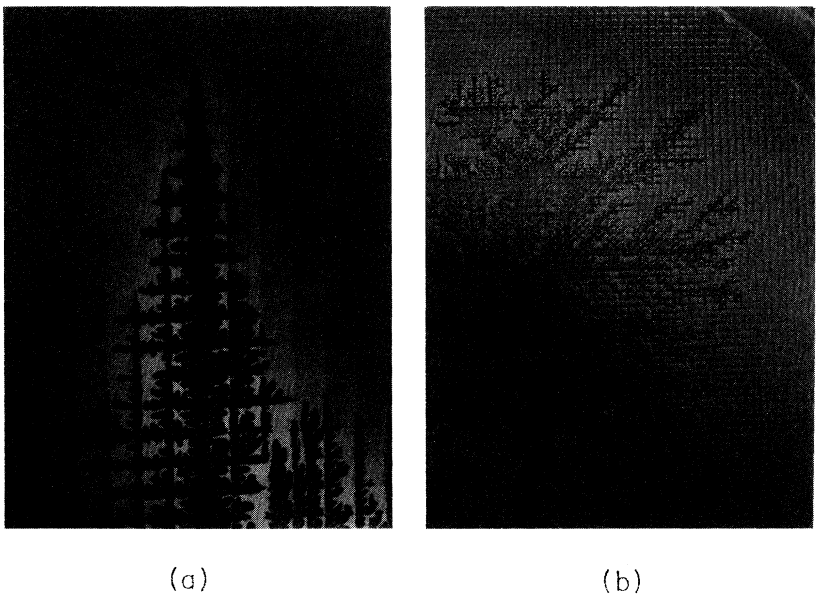

FIG. 10. The effect of the nature of the imposed anisotropy. (a) In this case, the stampings of the agar in the two perpendicular directions were of different durations, leading to a quasitwofold anisotropy. (b) The agar was stamped with squares (seen in the picture) leading to a branching growth.

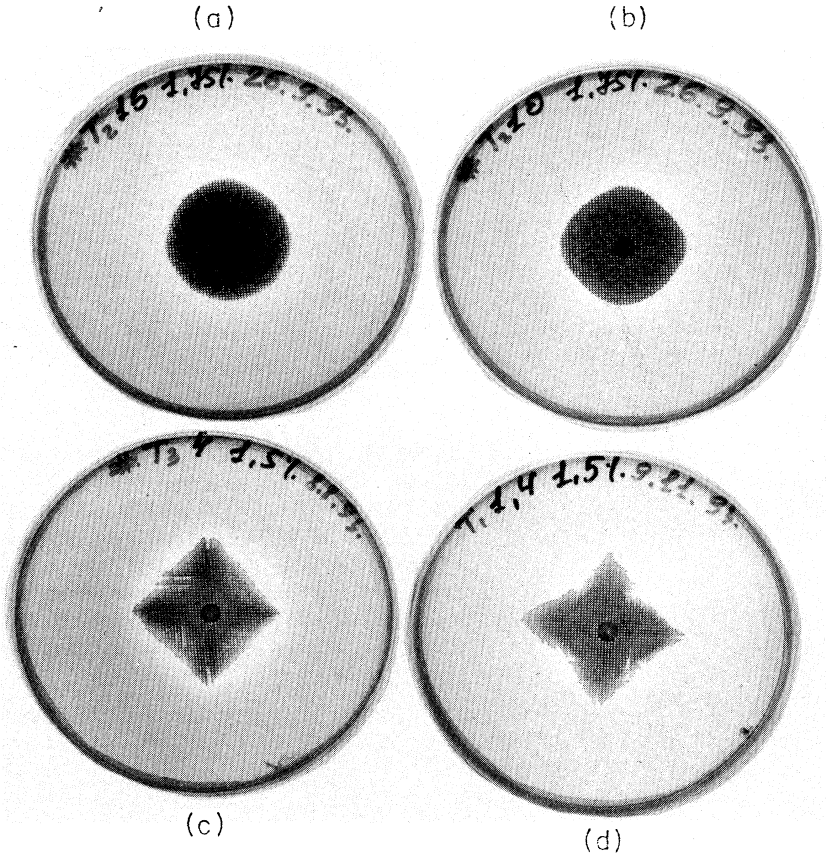

FIG. 11. Patterns observed during growth in the presence of imposed fourfold anisotropy for 1.5% agar. (a), (b), (c), and (d) are for peptone levels 15, 10, 4, and 1.4 g/l, respectively. Note the similarity to the model predictions shown in Fig. 4.

the imposed anisotropy. In Fig. 10(a) we show the effect when the anisotropy in one direction is more pronounced and in Fig. 10(b) we show the effect of a fourfold lattice of squares.

Following the theoretical predictions we have studied the growth as a function of peptone level (Fig. 11). A clear concave-to-convex transition is observed. The qualitative agreement with the model predictions indicates the predictive power of the communicating walkers model as well as the need to include repulsive chemotaxis signaling to capture the observed phenomena. The results also suggest that morphology transitions occur and hence a morphology selection principle acts during growth of the bacterial colonies.

ACKNOWLEDGMENTS

We are most thankful to Inna Brainis for growing the colonies presented here. We also thank Danny Weiss and Hermann Leibovich for technical assistance. We have benefited from conversations with Eliora Ron, Jim Shapiro, David Gutnick, David Kessler, Herbert Levine, and Peter Garik. This research was supported in part by a grant from the GIF, the German-Israeli Foundation for Scientific Research and Development, by Grant No. 9200051 from the United States–Israel Binational Science Foundation (BSF), by the Hungarian Research Foundation Grant No. T4439, and by the Program for Alternative Thinking at Tel-Aviv University.

[1] D. A. Kessler, J. Koplik, and H. Levine, Adv. Phys. **37**, 255 (1988).
[2] J. S. Langer, Science **243**, 1150 (1989).
[3] E. Ben-Jacob and P. Garik, Nature **343**, 523 (1990).
[4] E. Ben-Jacob, Contemp. Phys. **34**, 247 (1993).
[5] J. A. Shapiro, Sci. Am. **258** (6), 62 (1988).
[6] R. Y. Stainer, M. Doudoroff, and E. A. Adelberg, *The Microbial World* (Prentice-Hall, Inc., Englewood Cliffs, NJ, 1957).
[7] H. Fujikawa and M. Matsushita, J. Phys. Soc. Jpn. **58**, 3875 (1989).
[8] M. Matsushita and Fujikawa, Physica A **168**, 498 (1990).
[9] E. Ben-Jacob, H. Shmueli, O. Shochet, and A. Tenenbaum, Physica A **187**, 378 (1992).
[10] E. Ben-Jacob, A. Tenenbaum, O. Shochet, and O. Avidan, Physica A **202**, 1 (1994).
[11] T. Matsuyama, R. M. Harshey, and M. Matsushita, Fractals **1**, 302 (1993).
[12] T. Matsuyama and M. Matsushita, Crit. Rev. Microbiol. **19**, 117 (1993).
[13] E. Ben-Jacob, O. Shochet, A. Tenenbaum, and O. Avidan, in *Spatio-Temporal Patterns in Nonequilibrium*

Complex Systems, edited by P. E. Cladis and P. Palffy-Muhoray, Santa-Fe Institute Studies in the Sciences of Complexity (Addison-Wesley Publishing Company, Reading, MA, 1995), pp. 619–634.
[14] M. Matsushita, J.-I. Wakita, and T. Matsuyama, in *Spatio-Temporal Patterns in Nonequilibrium Complex Systems* [13] pp. 609–618.
[15] E. Ben-Jacob, O. Shochet, A. Tenenbaum, I. Cohen, A. Czirók, and T. Vicsek, Nature **368**, 46 (1994).
[16] E. Ben-Jacob, O. Shochet, A. Tenenbaum, I. Cohen, A. Czirók, and T. Vicsek, Fractals **2**, 15 (1994).
[17] J. Schindler and T. Rataj, Binary **4**, 66 (1992).
[18] J. A. Shapiro, *Sci. Am.* **258** (6), 62 (1988).
[19] E. O. Budrene and H. C. Berg, Nature **349**, 630 (1991).
[20] P. Devreotes, Science **245**, 1054 (1989).
[21] H. C. Berg, Nature **254**, 389 (1975).
[22] J. Adler, Science **166**, 1588 (1969).
[23] *Biology of the chemotatic response*, edited by J. M. Lackiie (Cambridge University Press, Cambridge, England, 1981).
[24] T. Vicsek, A. Czirók, E. Ben-Jacob, I. Cohen, O. Shochet, and A. Tenenbaum, Phys. Rev. Lett. **75**, 1226 (1995).
[25] E. Ben-Jacob, I. Cohen, O. Shochet, A. Czirók, and T. Vicsek, Phys. Rev. Lett. **75**, 2899 (1995).
[26] O. Shochet, K. Kassner, E. Ben-Jacob, S. G. Lipson and H. M. Müller-Krumbhaar, Physica A **181**, 136 (1992); **197**, 87 (1992).
[27] E. Ben-Jacob, I. Cohen, and A. Czirók, Fractals (to be published).
[28] E. Ben-Jacob, I. Cohen, O. Shochet, I. Aranson, H. Levine, and L. Tsimiring, Nature **373**, 566 (1995).
[29] E. Ben-Jacob and I. Cohen, in *Bacteria as Multicellular Organisms*, edited by J. A. Shapiro and M. Dwarkin (Oxford University Press, Oxford, in press).
[30] J. Adler, Science, **166** 1588 (1969).
[31] H. C. Berg and E. M. Purcell, Biophys. J. **20**, 193 (1977).
[32] E. Ben-Jacob, I. Cohen, and A. Czirók, in *Physics of Biological Systems* (Springer, Berlin, in press).
[33] O. Shochet, Phys. Rev. E. **49**, R3598 (1994).
[34] E. Ben-Jacob, R. Godbey, N. D. Goldenfeld, J. Koplik, H. Levine, T. Mueller, and L. M. Sander, Phys. Rev. Lett. **55**, 1315 (1985).
[35] V. Horvath, T. Vicsek, and J. Kertesz, Phys. Rev. A **35**, 2353 (1987).
[36] Y. Couder, O. Cardoso, D. Dupuy, P. Tavernier, and W. Thom, Europhys. Lett. **2**, 437 (1986).
[37] G. Zocchi, B. E. Shaw, A. Libchaber, and L. P. Kadanoff, Phys. Rev. A **36**, 1894 (1987).
[38] E. Brener and V. I. Melnikov, Adv. Phys. **40**, 53 (1991).
[39] T. Ihle and H. Müller-Krumbhaar, Phys. Rev. Lett. **70**, 3083 (1993).
[40] E. Brener, H. Müller-Krumbhaar, Y. Saito, and D. Temkin, Phys. Rev. E. **47**, 1151 (1993).
[41] R. Kupferman, O. Shochet, and E. Ben-Jacob, Phys. Rev. E. **50**, 1005 (1994).
[42] R. Kupferman, D. Kessler, and E. Ben-Jacob, Physica A **231**, 451 (1995).

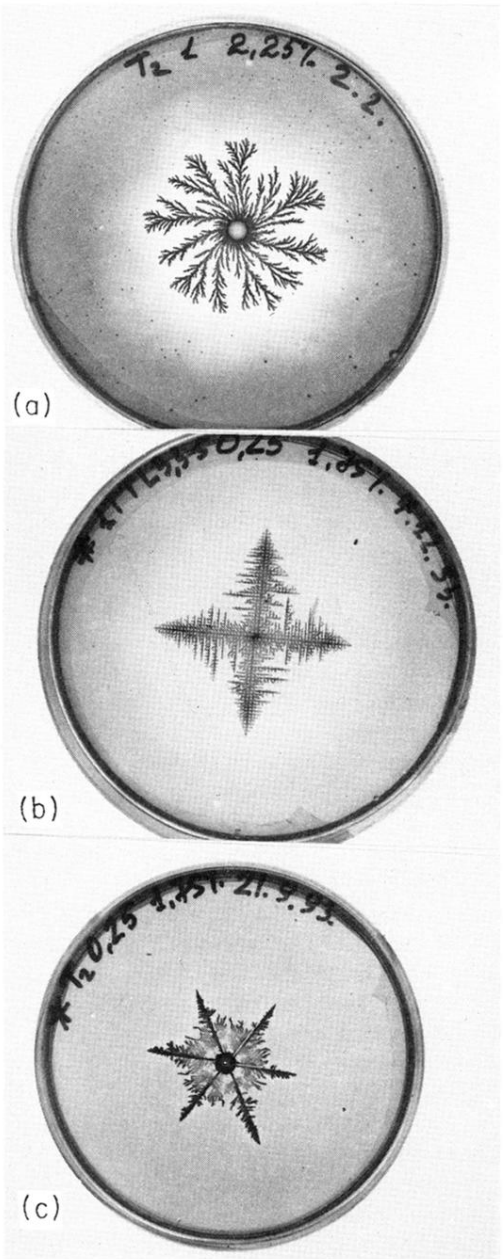

FIG. 1. The effect of imposed anisotropy. (a) Fractal growth in the absence of anisotropy on 2.25% agar (1% is 1 g per 100 ml) and 1 g/l peptone level. (b) Dendritic growth in the presence of imposed fourfold lattice anisotropy. The anisotropy is introduced using the "stamping" method described in the text. The growth is for 0.25 g/l peptone level and 1.75% agar concentration. Note the dramatic effect of the imposed anisotropy and the tantalizing similarity to solidification patterns and patterns produced in Hele-Shaw experiments. (c) "Bacterial snowflake," the same as (b) but in the presence of sixfold anisotropy.

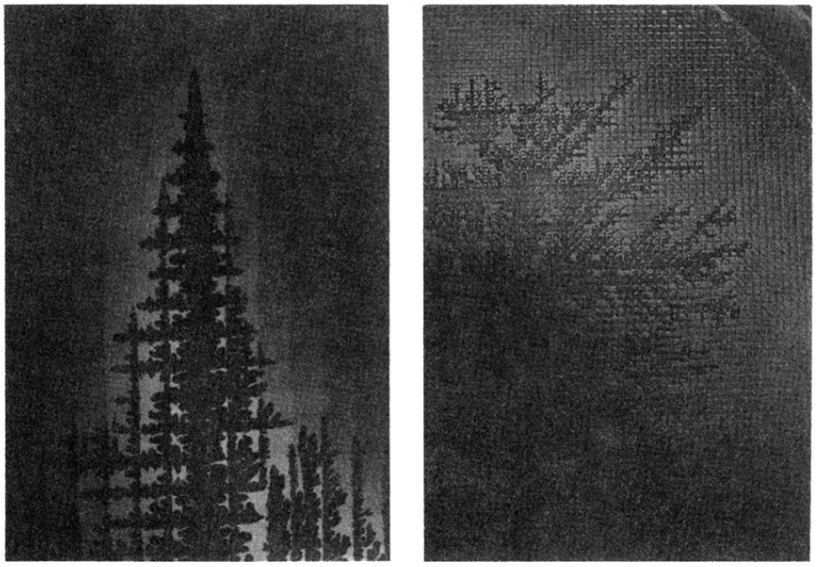

(a) (b)

FIG. 10. The effect of the nature of the imposed anisotropy. (a) In this case, the stampings of the agar in the two perpendicular directions were of different durations, leading to a quasitwofold anisotropy. (b) The agar was stamped with squares (seen in the picture) leading to a branching growth.

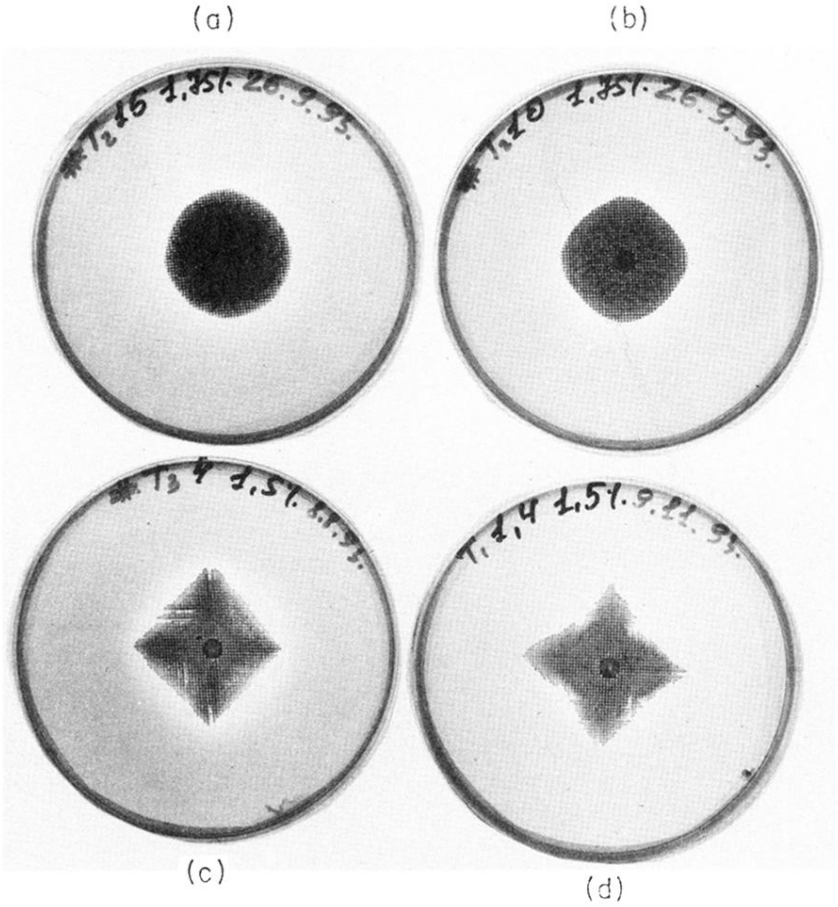

FIG. 11. Patterns observed during growth in the presence of imposed four-fold anisotropy for 1.5% agar. (a), (b), (c), and (d) are for peptone levels 15, 10, 4, and 1.4 g/l, respectively. Note the similarity to the model predictions shown in Fig. 4.

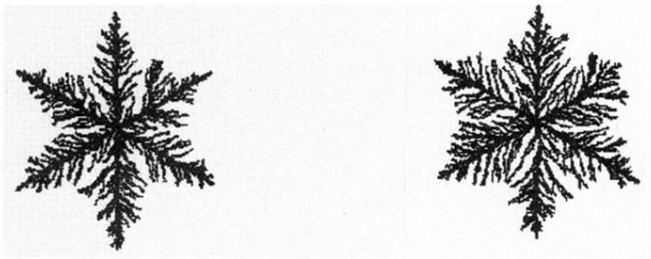

FIG. 3. The effect of repulsive chemotaxis. (a) and (b) are the same as Fig. 2(d) but with repulsive chemotaxis [stronger in (b)]. The pattern becomes dense and the anisotropy is retained.

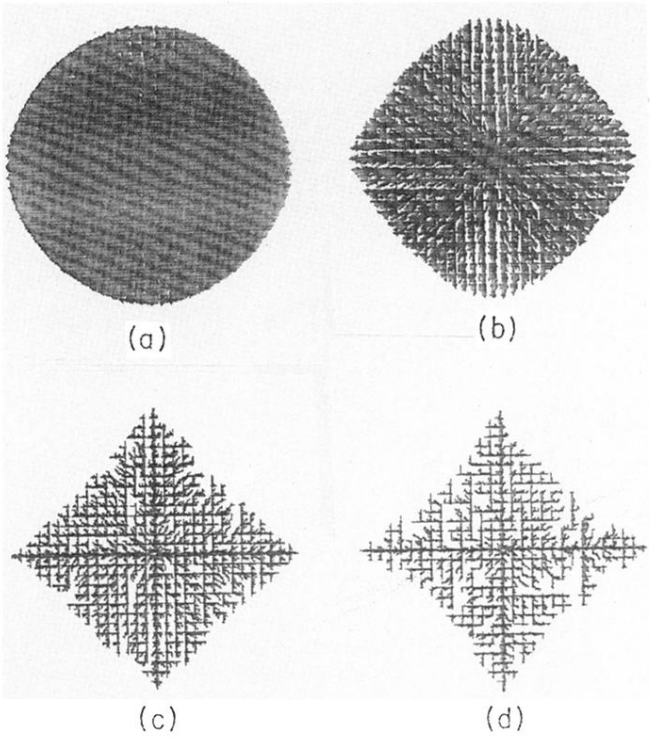

FIG. 4. Patterns produced by the "communicating walkers" model in the presence of lattice fourfold anisotropy and with chemotaxis signaling. The simulations are for N_c=20. (a)–(d) are for P=75, 35, 15, and 10, respectively. Note that the envelope shows a transition from concave to convex shape envelope.

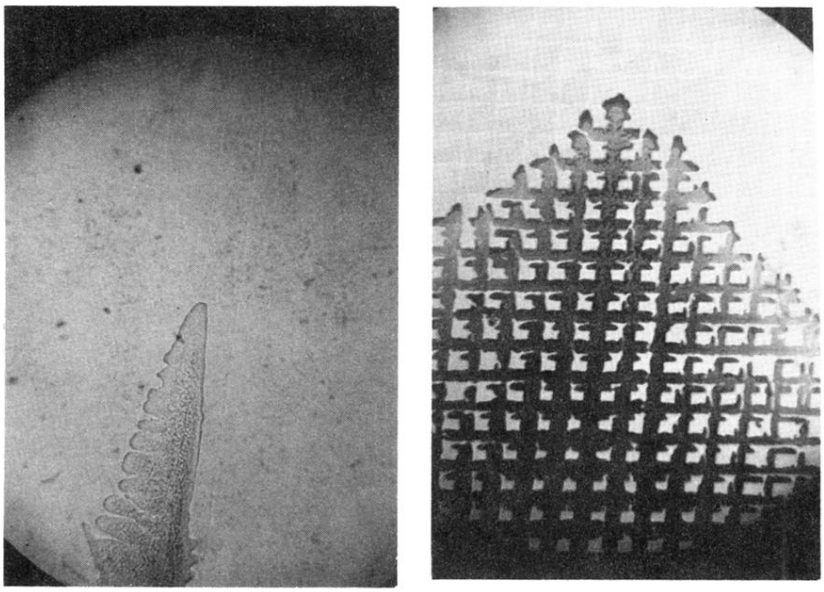

FIG. 5. Close-up picture of the imposed anisotropy ($\times$ 50 magnification) showing the marks left on the agar. (a) Imposed sixfold anisotropy. A segment of one of the six lines is shown. In this case the agar was stamped with wide channels (about 0.6 mm) leading to the growth of parity-broken dendrites (see text). (b) Imposed fourfold mesh anisotropy.

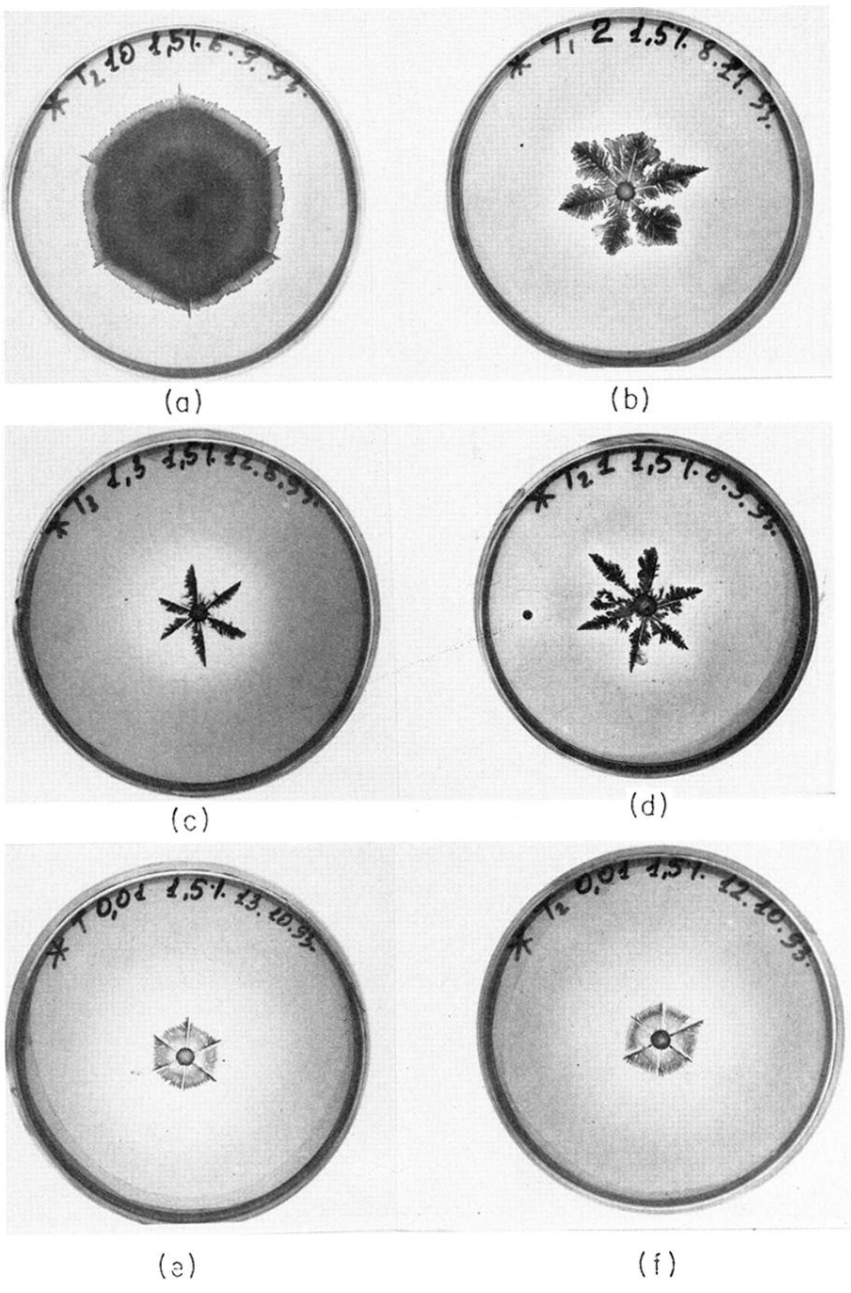

FIG. 6. Patterns observed during growth in the presence of sixfold anisotropy on 1.5% agar concentration and for 10, 2, 1.3, 1.0, 0.01, and 0.01 g/l peptone levels for (a), (b), (c), (d), (e), and (f), respectively. Note that the patterns become denser again at very low peptone levels. The patterns in (e) and (f) (both for the same growth conditions) demonstrate the reproducibility of our results when a strict protocol is followed.

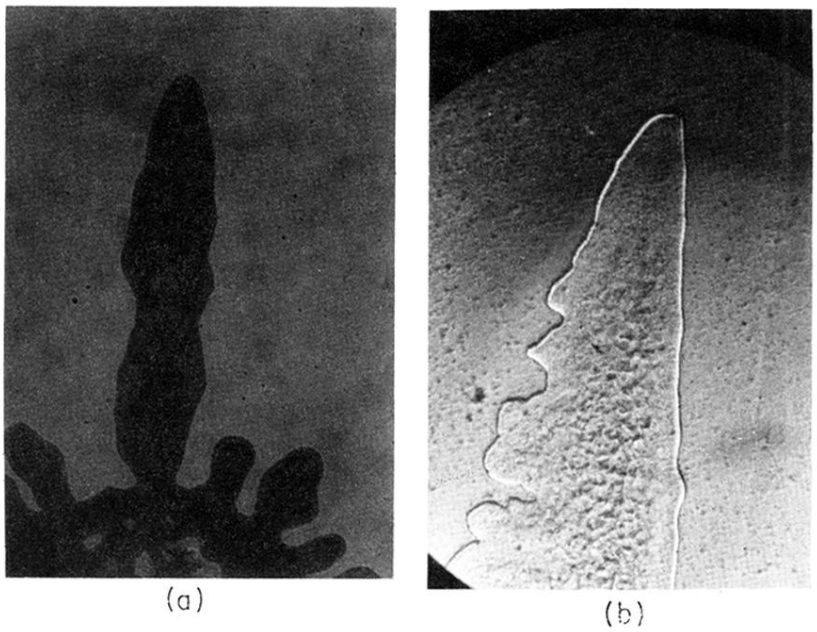

FIG. 7. Close-up look ($\times$ 50 magnification) at dendritic growth. (a) Ordinary dendrite with parabolic tip (growth in the presence of twofold anisotropy). (b) Parity-broken dendrite (in the presence of sixfold anisotropy). Note that it appears as "half" of an ordinary dendrite.

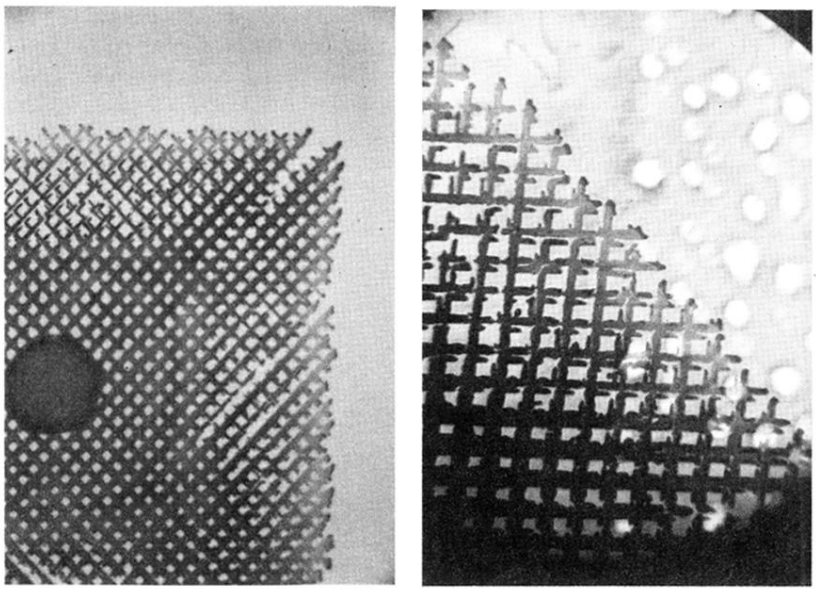

(a) (b)

FIG. 8. "Bacterial crystals": growth in the presence of fourfold anisotropy. Note the well defined envelope of the growth. (b) Shows a close look at a segment of (a).

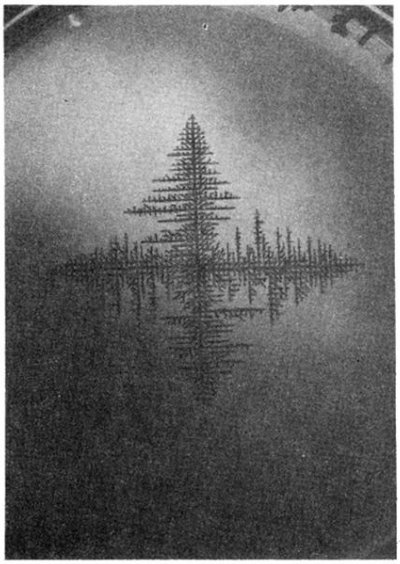

(a)

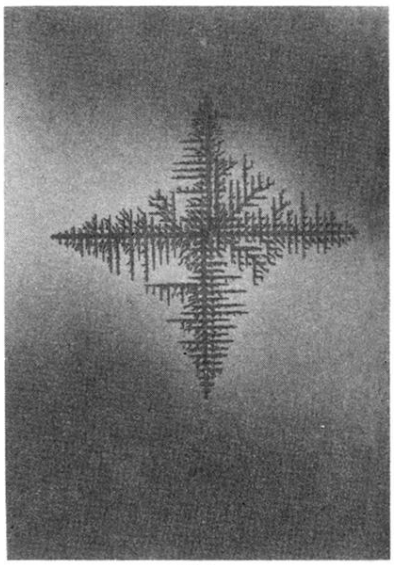

(b)

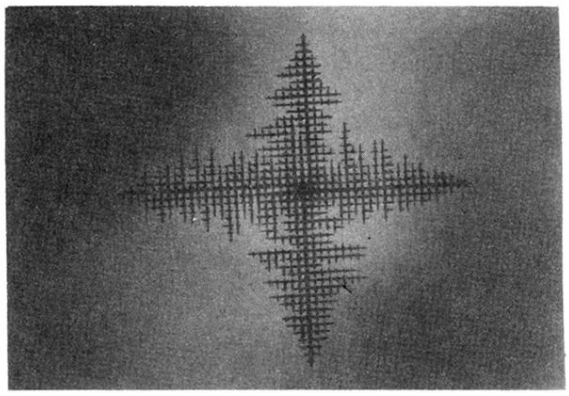

(c)

FIG. 9. Demonstration of the reproducibility in the observations. (a), (b), and (c) are for 1.75% agar concentration and 0.25 g/l peptone level. The differences in size are an artifact of the photography. The actual size is the same in all three cases. Note the transient effects near the center of the growth which are due to the initial inoculation (by picking in the center).